Materials Science & Engineering A 648 (2015) 51–56

Contents lists available at ScienceDirect

Materials Science & Engineering A

journal homepage: www.elsevier.com/locate/msea

Combination of ductility and toughness by the design of fine ferrite/tempered martensite–austenite microstructure in a low carbon medium manganese alloyed steel plate

Jun Chen [a,*], Meng-yang Lv [b], Zhen-yu Liu [a], Guo-dong Wang [a]

[a] State Key Laboratory of Rolling and Automation, Northeastern University, Shenyang 110819, People's Republic of China
[b] School of Materials and Metallurgy, Northeastern University, Shenyang 110819, People's Republic of China

ARTICLE INFO

Article history:
Received 13 June 2015
Received in revised form
6 September 2015
Accepted 8 September 2015
Available online 11 September 2015

Keywords:
Medium manganese steel
Retained austenite
Strain hardening behavior
Mechanical properties

ABSTRACT

Based on the mechanisms of plasticity and toughness, a low carbon medium manganese alloyed steel plate with the outstanding combination of ductility and toughness was designed. The microstructure characteristics, strain hardening behavior and toughening mechanisms were investigated in detail. The microstructure is composed of ferrite/tempered martensite and austenite after heat treating at 650 °C for 2 h. The retained austenite shows multi-type morphology, multi-scale size and relatively poor mechanical stability, resulting in multi-peak strain hardening behavior and sufficient TRIP effect. The excellent strain hardening capacity and ductility are hence achieved. The excellent low temperature toughness is also achieved due to the relatively lower concentrations of Mn and C, the formation of fine ferrite grains and a small volume fraction of fine retained austenite. The steel hence possesses the excellent ductility (the total elongation is ~37.3%) and low temperature toughness (the Charpy V-notch impact energy is ~158 J at −80 °C).

1. Introduction

Recently, medium Mn transformation induced plasticity (TRIP) steels containing 5–8 mass% Mn have been attracting more attentions due to the outstanding combination of strength and ductility [1–8]. Moreover, Since Miller proposed 0.11C–5.7Mn steel [9], the reverse transformation behavior, stabilization mechanisms of retained austenite, strain hardening behavior and tensile properties had been further understood [1–4,9–14]. It has been recognized that only sufficiently stable retained austenite in general leads to strong toughening [15,16]. Whereas the high stable retained austenite has few contributions to strain hardening capacity, resulting in the dramatic reduction in ductility. The role of retained austenite in improving ductility and toughness is inconsistent. However, it has been demonstrated that the high strain hardening capacity and ductility can be effectively enhanced by the TRIP effect. The sufficient TRIP effect of metastable austenite indicates that its contribution to low temperature toughness is very poor. Hence, some other toughening mechanisms should be introduced. It is well known that the Mn and C are strong austenite stabilizers and the volume fraction and stability of retained austenite increase with increasing the concentrations of Mn and C [4,10,14], resulting in the attractive strain hardening capacity and ductility. However, the high Mn and C steels with a body-centered cubic crystal structure always have relatively high ductile brittle transition temperatures [17]. Therefore, the Mn and C concentrations should be reduced. On the other hand, we also add some Ni and refine grains to enhance toughness.

The objective of the present work was therefore to investigate whether the excellent combination of ductility and low temperature toughness can be achieved by the design of fine ferrite/tempered martensite–austenite microstructure in a low carbon medium manganese alloyed steel plate. Particular attentions were to elucidate strain hardening behavior and toughening mechanisms. This study was done by a quantitative analysis of the morphology and size of retained austenite.

2. Experimental procedure

The chemical composition of the steel is Fe–0.05C–0.23Si–3.3Mn–0.003P–0.001S–1.4Ni (in mass%), which has relatively lower Mn and C concentrations by comparison with other medium manganese steels. The steel was melted by means of a high-frequency vacuum induction furnace in an Ar protective atmosphere and cast into an iron mold. The ingot was homogenized at 1200 °C

* Corresponding author. Fax: +86 24 2390 6472.
E-mail address: cjer19841011@163.com (J. Chen).

http://dx.doi.org/10.1016/j.msea.2015.09.032
0921-5093/

for 2 h, then hot rolled in six passes to a 12 mm thickness plate, and finally cooled to room temperature in water. The plate was further isothermally treated at 650 °C for 2 h to obtain a considerable volume fraction of retained austenite, and then water quenched to room temperature.

Standard round tensile samples with the gauge length of 40 mm and diameter of 8 mm were sampled from above mentioned tempered steel plate along the rolling direction. Interrupted tensile tests were conducted on a CMT-5105 tensile tester at room temperature at a cross beam speed of 3 mm/min. The standard Charpy V-notch (CVN) impact samples with the size of 10 × 10 × 55 mm^3 were also prepared along the rolling direction, and the impact tests were conducted on a JBW-500 impact tester at the temperatures of 15, −40 and −80 °C. Moreover, the average yield strength, ultimate tensile strength, total elongation and CVN impact energy were determined using three tensile or CVN impact test data.

Specimens were cut from the tempered steel plate and their surfaces along thickness direction and rolling direction were mechanically polished and then etched in 4% nital solution for optical microscopy (OM, LEICA DMIRM) and scanning electron microscopy (SEM, Zeiss Ultra 55). The quantitative X-ray diffraction (XRD) analysis was used to determine the volume fractions of retained austenite. Meanwhile, for accurate measurement, the specimens were cut from the gauge section of different tensile samples with different strains, mechanically polished, and then electropolished in a mixture consisting of ~12.5% perchloric acid and ~87.5% absolute ethyl alcohol at room temperature to remove surface strain layer. Furthermore, the volume fractions of retained austenite were measured using the integrated intensities of $(200)_\gamma$, $(220)_\gamma$, $(113)_\gamma$, $(200)_\alpha$, $(112)_\alpha$ and $(220)_\alpha$ diffraction peaks [18,19]. Transmission electron microscopy (TEM) specimens were mechanically thinned to ~50 μm thickness from both sides using silica papers, followed by punching to prepare round disks with 3 mm diameter. Subsequently, the disks were further thinned using a twin-jet electropolisher (Struers TenuPol-5) under a voltage of ~32 V at a temperature of ~−10 °C. The electrolyte consisted of ~9% perchloric acid and ~91% absolute ethyl alcohol. The thin foils were examined on a field-emission transmission electron microscopy (FEI Tecnai G^2 F20) operated at 200 kV and well investigated using selected area electron diffraction (SAED).

3. Results and discussion

3.1. Mechanical properties and multi-peak strain hardening behavior

The true stress–strain curve and the corresponding strain hardening rate of the steel are shown in Fig. 1. The steel shows an ultimate tensile strength (UTS) of ~763 MPa, lower yield strength of ~530 MPa and total elongation (TE) of ~37.3%, exhibiting a low yield ratio of ~0.69 and superior combination of UTS and TE. It is interesting to note that the clear steps (indicated as A to G in the inset in Fig. 1a) in true stress–strain curve are visible below the true strain of 0.08. Beyond this point, the true stress continuously increases as the true strain increases. On the other hand, the strain hardening rate was derived from the true stress–strain curve, as shown in Fig. 1b, exhibiting that many peaks in strain hardening rate curve are observed and the peak value is far higher than that reported in previous studies [20,21]. A steep increase in true stress

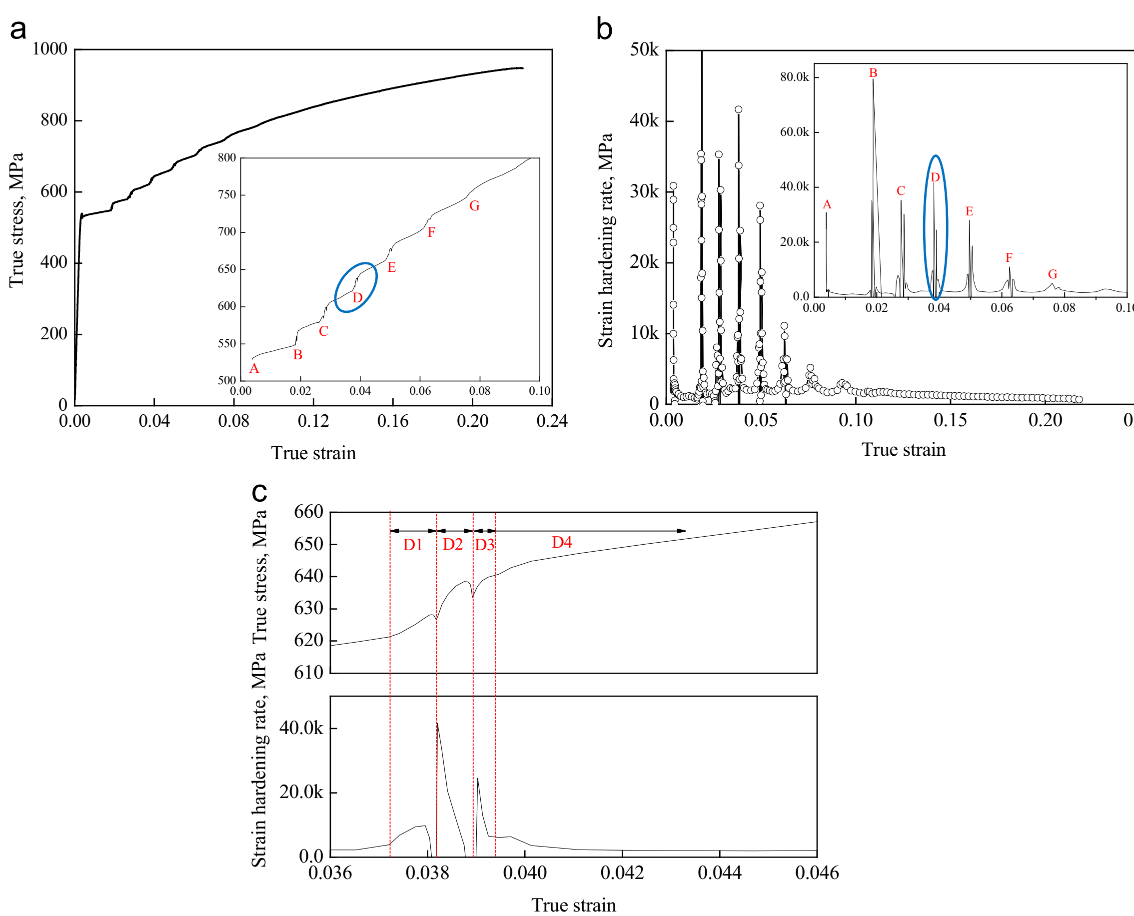

Fig. 1. Tensile stress–strain curve and corresponding strain hardening rate curve of the steel. (a) True stress–strain curve; (b) multi-peak strain hardening behavior and (c) local magnification map taken from representative region D.